Chemical Physics 456 (2015) 13–21

Contents lists available at ScienceDirect

Chemical Physics

journal homepage: www.elsevier.com/locate/chemphys

Probing the structures and electronic properties of dual-phosphorus-doped gold cluster anions ($Au_nP_2^-$, n = 1–8): A density functional theory investigation

Kang-Ming Xu [a], Teng Huang [a], Yi-Rong Liu [a], Shuai Jiang [a], Yang Zhang [a], Yu-Zhou Lv [a], Yan-Bo Gai [a], Wei Huang [a,b,*]

[a] Laboratory of Atmospheric Physico-Chemistry, Anhui Institute of Optics and Fine Mechanics, Chinese Academy of Science, Hefei, Anhui 230031, China
[b] School of Environmental Science and Optoelectronic Technology, University of Science and Technology of China, Hefei, Anhui 230026, China

ARTICLE INFO

Article history:
Received 25 March 2015
In final form 29 April 2015
Available online 8 May 2015

Keyword:
Gold cluster
Phosphorus
DFT
Electronic property

ABSTRACT

The geometries of gold clusters doped with two phosphorus atoms, $Au_nP_2^-$ (n = 1–8), were investigated using density functional theory (DFT) methods. Various two-dimensional (2D) and three-dimensional (3D) structures of the doped clusters were studied. The results indicate that the structures of dual-phosphorus-doped gold clusters exhibit large differences from those of pure gold clusters with small cluster sizes. In our study, as for $Au_6P_2^-$, two cis–trans isomers were found. The global minimum of $Au_8P_2^-$ presents a similar configuration to that of Au_{20}^-, a pyramid-shaped unit, and the potential novel optical and catalytic properties of this structure warrant further attention. The higher stability of $Au_nP_2^-$ clusters relative to Au_{n+2}^- (n = 1–8) clusters was verified based on various energy parameters, and the results indicate that the phosphorus atom can improve the stabilities of the gold clusters. We then explored the evolutionary path of $Au_nP_2^-$ (n = 1–8) clusters. We found that $Au_nP_2^-$ clusters exhibit the 2D–3D structural transition at n = 6, which is much clearer and faster than that of pure gold clusters and single-phosphorus-doped clusters. The electronic properties of $Au_nP_2^-$ (n = 1–8) were then investigated. The photoelectron spectra provide additional fundamental information on the structures and molecular orbitals shed light on the evolution of $Au_nP_2^-$ (n = 1–8). Natural bond orbital (NBO) described the charge distribution in stabilizing structures and revealed the strong relativistic effects of the gold atoms.

1. Introduction

Gold is an element whose unique properties are strongly influenced by relativistic effects [1–3]. Haruta [4] first reported that gold nano-clusters exhibit catalytic properties; since that report, the structures of gold nano-clusters have received considerable attention [1–3,5]. A series of experimental and theoretical studies have examined the unique structures and exciting properties of small-to-medium pure gold clusters [6–23]. Gold clusters doped with metal/nonmetal species have also been widely investigated based on the expectation that varying the dopant alters the size and shape of the clusters in addition to tailoring the properties of the nano-clusters [24–46].

Phosphorus-doped gold clusters have received significant attention, in part due to interest in understanding the fascinating properties of these materials, particularly their semiconductivity and unique optical properties [47,48]. A number of experimental [49–55] and theoretical [56–60] investigations have also been reported on the reactivities of gold clusters doped with phosphorus.

Jeitschko and Moller [49] investigated the Au–Au interaction in the crystal structure of the well-known Au_2P_3 structure. Eschen and Jeitschko [50] reported the network crystal structure of Au_2MP_2 (M = Pb, Tl, and Hg) in three dimensions with condensed 8-membered Au_2P_6 and 10-membered Au_4P_6 rings. Weizer and Fatemi [51] reported the contact resistance of a Au_2P_3 layer, which was found to be very sensitive to the growth rate of the interfacial Au_2P_3 layer. Henkes et al. [52] reported on Au_2P_3 and other metal phosphides synthesized using hot trioctylphosphine (TOP) as a solvent. A study on the generation of $Au_nP_m^{\pm}$ using a Nd:YAG (532 nm) laser was reported by Zheng and co-workers [53]. Recently, Panyala et al. [54] also studied $Au_nP_m^{\pm}$ clusters with different m

* Corresponding author at: Laboratory of Atmospheric Physico-Chemistry, Anhui Institute of Optics and Fine Mechanics, Chinese Academy of Science, Hefei, Anhui 230031, China.
E-mail address: huangwei6@ustc.edu.cn (W. Huang).

http://dx.doi.org/10.1016/j.chemphys.2015.04.019
0301-0104/

and n values using laser ablation coupled with TOF-MS, the new gold phosphides generated might inspire synthesis of new Au–P materials with specific properties. Carenco et al. [55] developed a versatile route for investigating the formation of Au_2P_3 nanostructures.

In contrast, there have been few theoretical studies on the structural and bonding properties of Au–P clusters using different calculation methods based on density functional theory (DFT) [57–60]. Theoretical studies on the electronic structures of Au_2MP_2 (M = Pb, Tl, and Hg) have been undertaken by Wen et al. [56]. Similar results have been reported by Eschen and Jeitschko [50] for the network crystal structure of Au_2MP_2 (M = Pb, Tl, and Hg). Li et al. [57] studied the geometries, stabilities, and electronic properties of neutral Au_nP_2 (n = 1–8) clusters, and Zhao et al. [58] reported findings for neutral Au_{12} clusters doped with secondary periodic elements based on DFT. The atomic and electronic structures of Au_5M (M = Na, Mg, Al, Si, P, and S) [60] and M@Au_6 (M = Al, Si, P, S, Cl, and Ar) [59] clusters have been investigated using DFT with a scalar relativistic effective core potential basis set. However, to the best of our knowledge, no systematic investigations of anionic phosphorus-doped gold clusters have been reported in the literature.

Herein, we report a density functional theory study of a series of small gold clusters doped with two phosphorus atoms ($Au_nP_2^-$ (n = 1–8)). This study is a follow-up to our previous work which focused on single-phosphorus-doped gold clusters [61]. We selected this size range to probe how isoelectronic substitutions affect the structures of pure gold clusters. We observed the two–three dimensional (2D–3D) structural transition at n = 6, which is earlier than that of pure gold clusters and much clearer than that of single-phosphorus-doped gold clusters (Au_nP^-), which show an even–odd oscillation in 2D/3D transition. The unique pyramid-shaped structure substitutes the planar Au_{10}^- cluster to afford the global minimum of $Au_8P_2^-$.

2. Theoretical methods

The basin-hopping (BH) global search method [62–66] coupled with DFT was employed to search for low-lying isomers of phosphorus-doped clusters of the type $Au_nP_2^-$ (n = 1–8). The original BH algorithm fundamentally combined the Metropolis random sampling technique and local optimization procedures. Two steps were included in this method: a new structure was generated via the random displacement of atoms and then optimized to the local minimum; this local energy minimum was used as a criterion to accept the initial generated structure spaces with the Boltzmann weight at a finite temperature. In our study, randomly produced structures of each species were used as the initial inputs for the BH search method, and 200 initial low-lying isomers were generated after 200–300 BH moves. Considering the inevitable errors of DFT methods when applied to total energy calculations, several additional techniques were chosen for the DFT optimization, including the generalized gradient approximation (GGA) in the Perdew–Burke–Ernzerhof (PBE) [67], *hybrid* generalized gradient approximation (*hybrid*-GGA) in the Becke 3-parameter exchange and the Lee–Yang–Parr correlation (B3LYP) [68–70] functional forms coupled with four basis sets [61]. As shown the selection and verification on the functional and basis set for Au/P systems, PBE functional coupled with CRENBL basis set used for Au and P was selected for the optimization calculations; all approaches were implemented in the NWCHEM 5.1.1 software package [71,72].

The top 10 isomers with relatively low energies were then selected for single-point energy calculations at the PBE0 [73]/CRENBL level of theory. Because of the strong relativistic effects of the gold atom, the spin orbit (SO) coupling effect [74] also must be considered for heavy atoms such as gold. The PBE0/CRENBL level and SO effects were carefully selected for the gold atom to achieve quantitative agreement between the experimental and theoretical PES spectra [64,75–79].

Simulated photoelectron spectra of the selected low-lying isomers were generated for comparison with the experimental data to further identify the $Au_nP_2^-$ (n = 1–8) clusters. The first vertical detachment energies (VDEs) of the anion clusters were calculated as the difference between the energies of the neutral and anionic species of each isomer. The binding energies of all deeper occupied orbitals were then added to the first VDE to simulate the detachment features of the valence electrons as a line spectrum. Each line in the obtained spectra was then fitted with a Gaussian width of 0.04 eV to obtain continuous spectra.

3. Results and discussion

This section consists of two parts: the geometric structures and the electronic properties. In the first part, we focus on the geometric structures of $Au_nP_2^-$ (n = 1–8) at the PBE0/CRENBL SO//PBE/CRENBL level of theory. The global minima of the species are explored. Next, we discuss the stabilities of these lowest-energy isomers. We also attempt to describe the possible evolutionary process of dual-phosphorus-doped gold clusters. In the second part of this section, the theoretically simulated photoelectron spectra of the low-lying isomers and the corresponding HOMO–LUMO gaps are discussed to support the first part of this section and the molecular orbital analysis. Finally, natural bond orbital (NBO) [80,81] provides intuitive information of the natural population analysis (NPA) [82] assigning atomic charge and the natural electron configuration (NEC) in the clusters.

3.1. Geometric structures

3.1.1. Low-lying structures

AuP_2^-: Two low-lying isomers of **AuP_2^-** at the PBE0/CRENBL SO level of theory are presented in Fig. 1. The global minimum (Isomer 1) of AuP_2^- is a C_s structure with a middle-positioned P atom, and the isomer prefers an obtuse angle ∠Au–P–P. The other isomer is an acute-triangle-shaped structure with a relatively high energy of 1.645 eV, which has a low probability of being the global minimum.

$Au_2P_2^-$: The global minimum of the $Au_2P_2^-$ cluster (Fig. 1) is an axe-like structure (C_s), the same configuration of the major isomer of Au_3P^- in our previous study [61]. Isomer 2 (D_{2h}) is a high-symmetry structure with a 0.929 eV higher energy than the Isomer 1. The difference between Isomers 3 (C_s) and 4 (C_{2v}) lies in the Au–Au bond of Isomer 3. Isomer 5, as well as Isomers 2–4, with a greater energy difference than Isomer 1, shows a low probability of being the global minimum. The global minimum of the anion ($Au_2P_2^-$) differs somewhat from the neutral configuration (Au_2P_2) reported by Li et al. [57], which is expected because of the interaction of an additional electron in the structures [40,57,83,84].

$Au_3P_2^-$: The first five low-lying isomers of which possess a P–P bond are presented in Fig. 1. The lowest-energy isomer (Isomer 1) is a pentagon structure with an inner Au–Au bond. Isomer 2 is a zigzag structure evolved from the global minimum of $Au_2P_2^-$ by bonding an additional Au atom to the edge-positioned P atom. However, the energy of this isomer is considerably higher than Isomer 1. Different with Isomer 2, Isomer 3 evolves from the global minimum of $Au_2P_2^-$ by adding the extra Au atom on the same side of the P–P bond with its energy a slightly higher than Isomer 2. Isomer 4 has an hourglass-like structure, and the energy of this isomer is 0.677 eV greater than that of Isomer 1. Additionally, the energy of Isomer 5, in which all 3 gold atoms are linearly bonded,

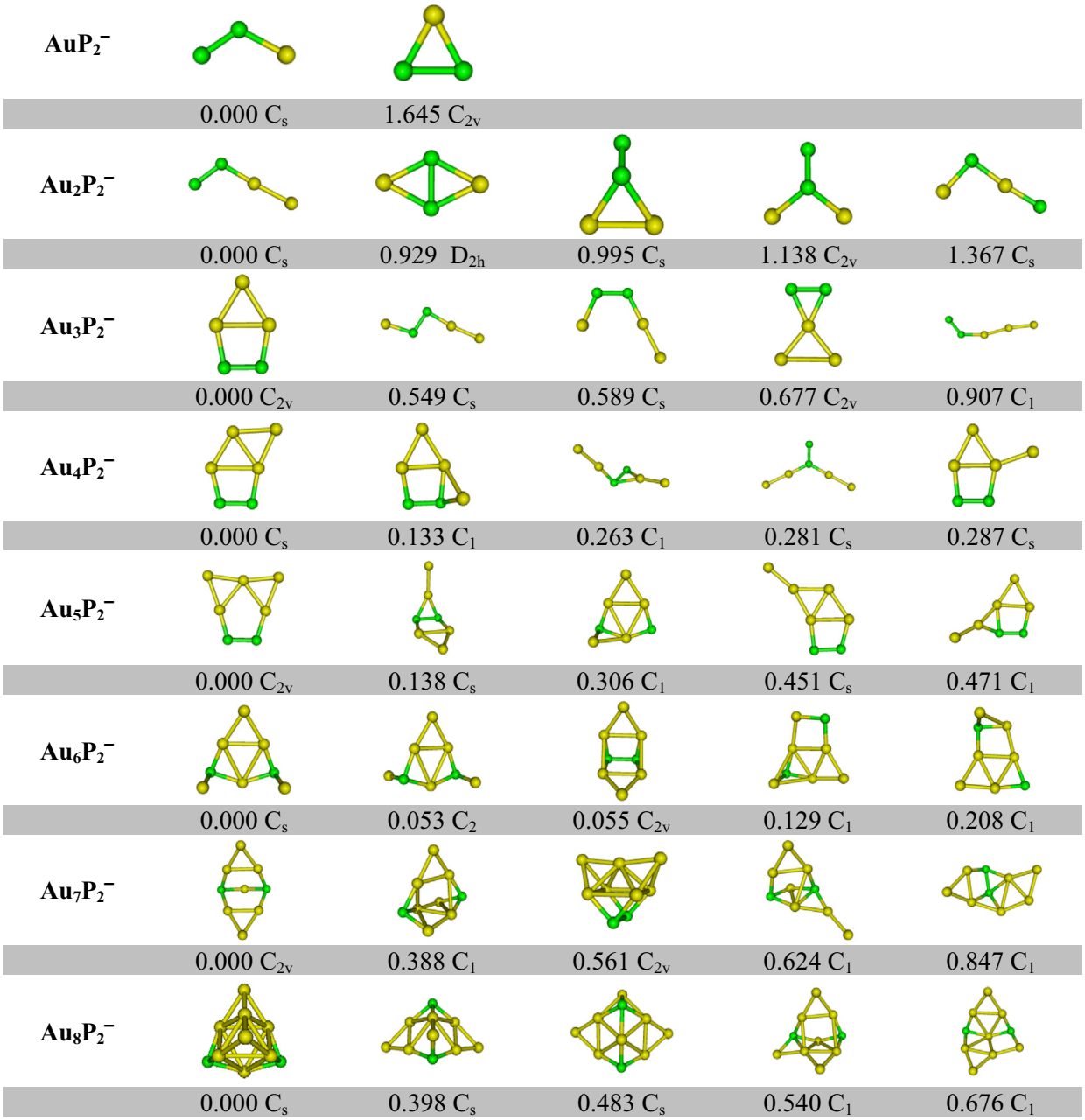

Fig. 1. The possible structural isomers, relative energies and molecular geometry symmetries of the low-lying isomers of $Au_nP_2^-$ (n = 1–8) at the PBE0/CRENBL level of theory.[1]

is 0.907 eV greater than that of Isomer 1. Isomers 2–5 are also unlikely to be the global minimum. The low isomers of $Au_3P_2^-$ are much different with that of the meta-stable phase of $Au_2P_3^-$ [84].

$Au_4P_2^-$: For $Au_4P_2^-$ in Fig. 1, the global minimum for the species is a planar structure (C_s). The isomer can clearly be envisioned as resulting from the attachment of an additional gold atom to the pentagon structure of $Au_3P_2^-$. Isomer 2 is 0.133 eV higher than Isomer 1 as a result of moving the Au atom from the upper right corner to the lower right corner. Isomers 3, 4, and 5 are unlikely to be the global minimum structures due to their relatively high energies. Isomer 5 and Isomer 1 differ by only one Au–Au bond; however, the 0.287 eV energy difference affords Isomer 5 with a low probability of being the most stable structure.

$Au_5P_2^-$: The global minimum is a planar structure (C_{2v}) with an additional Au atom added to the upper left corner of $Au_4P_2^-$ shown in Fig. 1. Isomer 2 can be viewed as a P–P bond dividing the 5 gold atoms into two parts. Isomer 3 differs from the other four top-5 isomers in the separation of the two phosphorus atoms of the structure. Isomer 3 is very similar to the global minimum of Au_6P^-, and the only difference is that a phosphorus atom substitutes a gold atom on the vertex. Isomers 4 and 5 can easily evolve from the first two low-lying isomers of $Au_4P_2^-$.

$Au_6P_2^-$: As shown in Fig. 1, there are two co-existing low-lying isomers for $Au_6P_2^-$. Two dangling Au atoms bond with one phosphorus atom. The difference between the two isomers lies in the relative position of the two dangling gold atoms. We refer to Isomers 1 and 2 as the "cis-isomer" and "trans-isomer", respectively, borrowing from the molecular naming rules of organic chemistry. The energy of the cis-isomer is slightly lower than that of the trans-isomer. Seven other density functional theory methods

[1] The top-5 isomers are ranked according to their relative energies for $Au_nP_2^-$ (n = 2–8), whereas the top-2 isomers are ranked for AuP_2^-.

also confirm the energy rankings of the two isomers (Table S1, Supplementary material). Isomer 3 is a C_{2v} structure, and its energy is also within 0.1 eV. Thus, it may be a local minimum. Isomers 4 and 5 exhibit a unique phenomenon in which one gold atom interacts with different phosphorus atoms of the quasi-planar Au_5P_2 base. The energy difference between Isomer 4 and Isomer 5 is large due to the different positions of the gold atoms.

$Au_7P_2^-$: The global minimum is a C_{2v} structure at the PBE0/CRENBL level in our study (Fig. 1). It is an irregular olive-shaped structure with a 1–2–3–2–1 formation ranked according to the number of atoms from the top to the bottom of the structure. Two phosphorus atoms are separated by a gold atom. Isomer 2 is a sailboat-type structure with two phosphorus atoms located at both ends of the sailboat. The structure is slightly distorted, and its energy is somewhat higher than that of Isomer 1. Isomer 3 is a quasi-tetrahedron-type structure, and the clear 3-layer structure makes it highly symmetrical. Isomers 4 and 5 are somewhat disordered structures.

$Au_8P_2^-$: It is very interesting that the global minimum of $Au_8P_2^-$ in our study is a pyramid-shaped structure, as shown in Fig. 1. The structure will exhibit very high symmetry if the two phosphorus atoms are substituted by gold atoms. Unfortunately, previous studies [7,8,11] have already reported that the global minimum of the Au_{10}^- cluster is a planar structure, whereas the Au_{20}^- cluster was confirmed to be a 4-layer pyramid-shaped (Td) structure with high chemical inertia and potential novel optical and catalytic properties [11]. This structure may be a basic unit for a large cluster configuration, which requires further exploration. Isomers 2 and 3 can be easily envisioned as resulting from substituting one gold atom for the phosphorus at the corresponding position. Both Isomer 4 and Isomer 5 have a relatively large energy difference from the lowest-energy isomer and are not common structures of $Au_8P_2^-$.

3.1.2. Relative stabilities

To predict the relative stabilities of the $Au_nP_2^-$ (n = 1–8) clusters, the average atomic binding energies E_b, dissociation energies Δ_1E, and the second-order difference of energies Δ_2E for the global minima are examined. The global minima of Au_{n+2}^- (n = 1–8) (Fig. S1, Supplementary material) are used for comparison. For the $Au_nP_2^-$ clusters, E_b, Δ_1E, and Δ_2E are defined as functions of the number of gold atoms n as follows:

$$E_b(n) = \left[(n-1)E(\mathrm{Au}) + 2E(\mathrm{P}) + E(\mathrm{Au}^-) - E(\mathrm{Au}_n\mathrm{P}_2^-)\right]/(n+2) \quad (1)$$

$$\Delta_1E(n) = E(\mathrm{Au}_{n-1}\mathrm{P}_2^-) + E(\mathrm{Au}) - E(\mathrm{Au}_n\mathrm{P}_2^-) \quad (2)$$

$$\Delta_2E(n) = E(\mathrm{Au}_{n-1}\mathrm{P}_2^-) + E(\mathrm{Au}_{n+1}\mathrm{P}_2^-) - 2E(\mathrm{Au}_n\mathrm{P}_2^-) \quad (3)$$

where E(Au), E(P), E(Au^-), E($Au_{n-1}P_2^-$), E($Au_nP_2^-$), and E($Au_{n+1}P_2^-$) denote the total energies of the Au, P, Au^-, $Au_{n-1}P_2^-$, $Au_nP_2^-$, and $Au_{n+1}P_2^-$ clusters, respectively. For the Au_n^- clusters, E_b, Δ_1E, and Δ_2E are defined as functions of the number of gold atoms n as follows:

$$E_b(n+2) = \left[(n+1)E(\mathrm{Au}) + E(\mathrm{Au}^-) - E(\mathrm{Au}_{n+2}^-)\right]/(n+2) \quad (4)$$

$$\Delta_1E(n+2) = E(\mathrm{Au}_{n+1}^-) + E(\mathrm{Au}) - E(\mathrm{Au}_{n+2}^-) \quad (5)$$

$$\Delta_2E(n+2) = E(\mathrm{Au}_{n+1}^-) + E(\mathrm{Au}_{n+2}^-) - 2E(\mathrm{Au}_{n+3}^-) \quad (6)$$

where E(Au), E(Au^-), E(Au_{n+1}^-), E(Au_{n+2}^-), and E(Au_{n+3}^-) denote the total energies of the Au, Au^-, Au_{n+1}^-, Au_{n+2}^-, and Au_{n+3}^- clusters, respectively.

The E_b, Δ_1E, and Δ_2E values of the lowest-energy structures for the $Au_nP_2^-$ and Au_{n+2}^- (n = 1–8) clusters versus the corresponding cluster size n are plotted in Fig. 2(a–c), respectively.

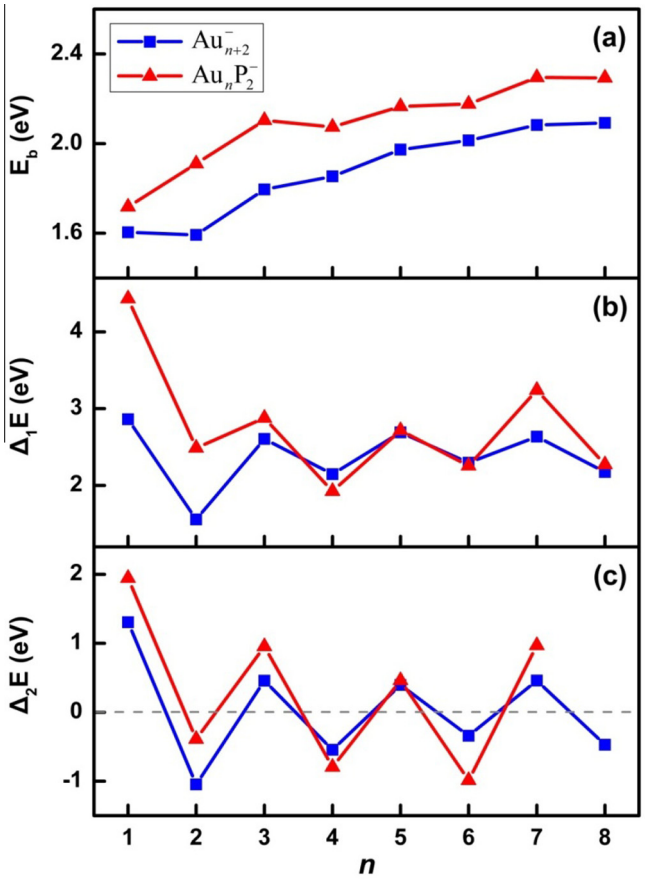

Fig. 2. Comparison of binding energies per atom E_b (a), dissociation energies Δ_1E (b), and the second-order difference of energies Δ_2E (c) of $Au_nP_2^-$ and Au_{n+2}^- as a function of cluster size. The results are obtained at the PBE/CRENBL level. (For interpretation of the references to color in this figure legend, the reader is referred to the web version of this article.)

As shown in Fig. 2(a), E_b of the $Au_nP_2^-$ clusters (red triangles) are higher than those of the Au_{n+2}^- clusters (blue blocks) at the same n value, indicating that the substitution of Au by P could improves the overall stability. The binding energy of two species of clusters generally increases with increasing cluster size (n), which could explain for the stabilities increase as the clusters size increasing.

Δ_1E represents the difficulty with which one Au atom is removed from the clusters, the higher the value is, the more stable the structure will be. Fig. 2(b) shows that Δ_1E of the $Au_nP_2^-$ (n = 1–8) clusters exhibits an odd–even oscillation as well as pure gold clusters [42,85]. It is more difficult to remove one gold atom from $Au_nP_2^-$ (n = 1, 3, 5, 7) than from $Au_nP_2^-$ (n = 2, 4, 6, 8) or Au_{n+2}^-. This should be due to the clusters with odd n values have an even number of electrons, forming a closed-shell configuration affected by the odd–even electron pairing effect. Therefore, removing one Au atom from closed-shell structure is more difficult than the corresponding open-shell structure.

The odd–even effect considering the second-order difference in energies Δ_2E is also illustrated in Fig. 2(c). For clarity, we denote n + 2 by m; thus, formula (6) can also be presented as (7) based on formula (5).

$$\Delta_2E(m) = \Delta_1E(m) - \Delta_1E(m+1) \quad (m = n+2) \quad (7)$$

From formula (7), we can see that Δ_2E is the dissociation energy difference between the corresponding cluster and its next order by the sharp oscillation. This parameter provides information about the values evenly distributed on both sides of the zero axis.

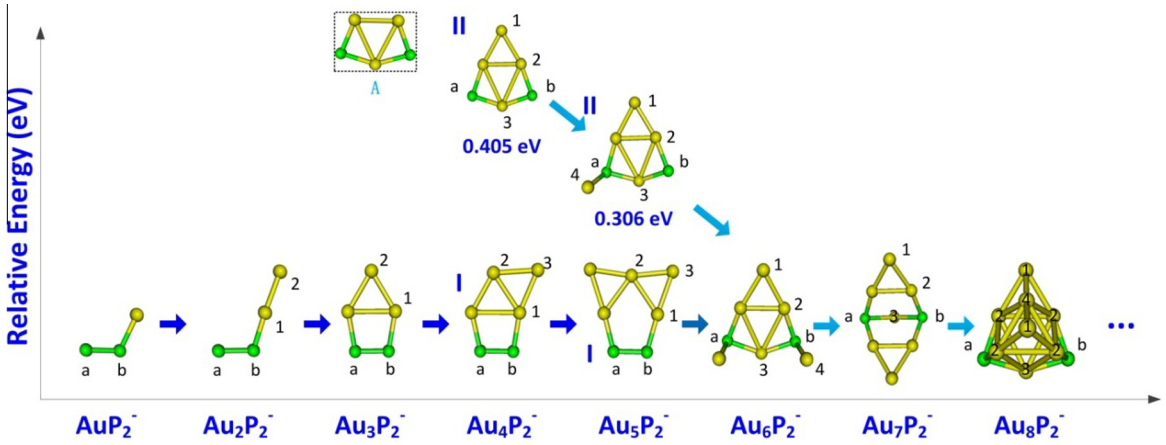

Fig. 3. Structural evolution of $Au_nP_2^-$ (n = 1–8). Digits represent different gold atoms, and letters of the alphabet represent different phosphorus atoms. Capital Roman numerals represent different isomers in the figure.

Odd-numbered Au atomic clusters possess positive values, whereas even-numbered clusters possess negative values. The definition illustrated in Eqs. (6) and (7) indicates that clusters with positive Δ_2E values are more stable.

3.1.3. Evolution of the structures

Fig. 3 shows a possible evolutionary path from AuP_2^- to $Au_8P_2^-$ to identify a rule that governs the growth of small-to-medium dual-phosphorous-doped gold clusters.

As mentioned above, AuP_2^-, a C_{2v} symmetric structure, can easily evolve into $Au_2P_2^-$ by bonding an additional gold atom (labeled No. 2) to the original gold atom. The pentagon-shaped structure of $Au_3P_2^-$ can be obtained by attaching an additional Au (1) atom to Au (2) and P (a), forming a closed-loop structure. The global minimum of $Au_4P_2^-$ is also a planar structure, and it can be envisioned as the pentagon structure of $Au_3P_2^-$ with a Au (3) atom added at the corner of the isomer. The Au (3) atom bonds with Au (2) and one Au (1). The evolution path from $Au_4P_2^-$ to $Au_5P_2^-$ is apparent. An additional Au (3) atom is added to the upper left corner of $Au_4P_2^-$, yielding a C_{2v} symmetric structure. Noting that the Au (1)–Au (1) bond breaks due to the atomic interaction caused by the two Au (3) atoms at each side bonding with two Au (1) atoms, the interaction pulls the two Au (1) atoms away, breaking the Au (1)–Au (1) bond.

Beginning with $Au_6P_2^-$, a different path appeared to explain the evolutionary progress of the $Au_nP_2^-$ species. As shown in Fig. 3, the global minimum of $Au_6P_2^-$ is a 3D structure with two separated P atoms. The evolutionary path may trace back to the precursor, which is not the global minimum. Isomer (II) of $Au_5P_2^-$ is a dangling structure that is similar to the global minimum of Au_7P^- [61]. The isomer is 0.305 eV higher than the global minimum of $Au_6P_2^-$. This high-energy isomer may also evolve from $Au_4P_2^-$ (II) with a 0.405 eV energy difference, as shown in the figure. Unfortunately, the possible precursor for $Au_4P_2^-$ (II) (labeled A in Fig. 3) was not observed in our study, which may be responsible for the high instability of the desired structure. In this case, the P–P bond can lower the energies of the isomers for small $Au_nP_2^-$ clusters ($n \leqslant 5$). When n is small, phosphorus plays a significant role in the cluster. It is considerably easier to form a P–P double bond to stabilize the structure. As the cluster size increases, the isomer including separated P atoms gradually decreases in energy to reach the global minimum.

$Au_6P_2^-$ evolves into $Au_7P_2^-$ by the combination of two dangling gold atoms with one additional gold atom to form a quasi-dihedral-angle structure. With continued growth, $Au_7P_2^-$ bonds with an additional gold atom to transform the quasi-planar structure into a regular 3D structure. The global minimum of $Au_8P_2^-$ is an exciting pyramid-shaped structure, and it can be envisioned as the positioning of an additional Au (4) atom between the two Au (1) atoms, linking the quasi-dihedral structure to form a 3-layer pyramid-shaped structure. In general, the structure with higher symmetry will be more stable.

The global minimum of the pure Au_{10}^- cluster is a planar structure; however, two phosphorus dopant atoms provide this cluster with a 3D pyramid-shaped structure. This stable and small unit may exhibit some unique physical and chemical properties that require further investigation.

It is clear that the 3D global minimum appears from n = 6, after which the P–P bond breaks and each P atom bonds with three Au atoms. Compared with pure anionic gold clusters (Au_n^-), in which the 3D configuration appears at n = 12, and with single phosphorus gold clusters Au_nP^-, which exhibit the even–odd effect, the 2D–3D structural transition of $Au_nP_2^-$ is much clearer and faster, and the structure is more stable.

3.2. Electronic properties

3.2.1. Simulated photoelectron spectra and HOMO–LUMO gap

Fig. 4 shows simulated photoelectron spectra of the global minimum (Isomer 1) of $Au_nP_2^-$ (n = 1–8) at the PBE0/CRENBL SO//PBE/CRENBL level of theory. The global minimum of AuP_2^- exhibits low vertical detachment energy (VDE) and a large HOMO–LUMO gap. Isomer 1 of $Au_2P_2^-$ also exhibits a relative low VDE and a larger HOMO–LUMO. Isomer 1 of $Au_3P_2^-$ has three distinct isolated peaks, predicting the change of the configuration which is different from the formers mentioned above. Isomer 1 of $Au_4P_2^-$ shown in figure presents a scaled-down three peak compared with $Au_3P_2^-$ and suggests the internal relation on the configurations. Isomer 1 of $Au_5P_2^-$ has a somewhat large HOMO–LUMO gap, and the neutral structure of this complex is a high-stability candidate for the species. Different from above, $Au_6P_2^-$ have two co-existed lowest-lying isomers as the simulated photoelectron spectra are shown in Fig. 4 ($Au_6P_2^-$ (I) & (II)). Although the structures have only a slight difference in cis–trans location of one Au atom, the VDE values, HOMO–LUMO gaps are large differences for obvious distinction. Additionally, this result also confirms that the PES is sensitive function to the configuration. The global minimum of $Au_7P_2^-$ has a large VDE (4.04 eV, Table S2, Supplementary material) and five single peak indicating the high stability and different-typed atoms of the configuration, respectively. The PES of

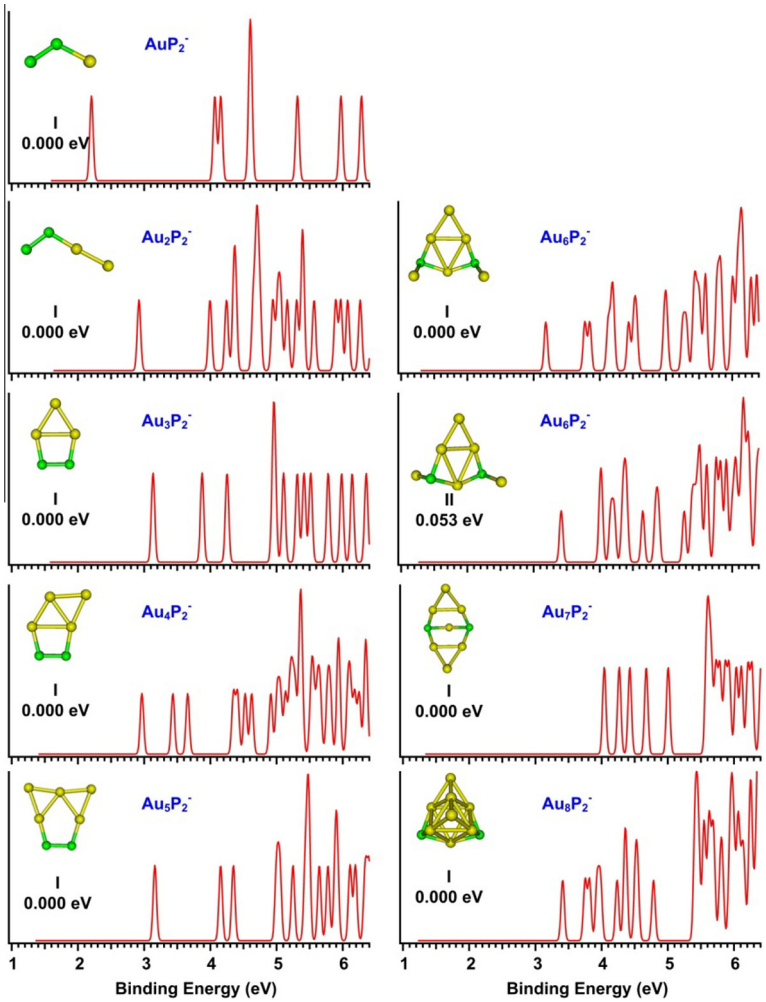

Fig. 4. Simulated photoelectron spectra of the global minimum of $Au_nP_2^-$ (n = 1–8) at the PBE0/CRENBL SO//PBE/CRENBL level of theory.

global minimum of $Au_8P_2^-$ shows a little complicated shape and the experimental PES data is necessary for confirming the global minimum of clusters.

3.2.2. Molecular orbital analysis

Fig. 5 shows the frontier molecular orbitals of the global minimum of each species of $Au_nP_2^-$ (n = 1–8). Selected information obtained from the figures is summarized below.

(1) $Au_2P_2^-$ & $Au_3P_2^-$, $Au_4P_2^-$ & $Au_5P_2^-$ and $Au_6P_2^-$ & $Au_7P_2^-$ can be treated as distinct groups because of their similar HOMO and LUMO values. This result indicates that the clusters of each group have similar orbital types. The precursor of each group is an open shell, whereas the later structure with an additional gold atom yields a closed shell with an even number of valence electrons. Hence, it is straightforward to transform from an open-shell cluster to a closed-shell cluster, with slight changes identified using molecular orbital theory. Meanwhile, a very large change is required to transform from the closed-shell structure of $Au_5P_2^-$ to the open-shell structure of $Au_6P_2^-$. The results of orbital hybridization indicate that the global minimum of $Au_6P_2^-$ does not have the lowest-energy isomer as its processor. This finding helps explain the change from $Au_5P_2^-$ to $Au_6P_2^-$.

(2) It was observed that closed-shell clusters, such as $Au_nP_2^-$ (n = 1, 3, 5, 7), add 10 molecular orbitals to the open-shell clusters, i.e., $Au_nP_2^-$ (n = 2, 4, 6, 8). In contrast, 9 orbitals were added when an open-shell structured transitioned to a closed-shell structure. It is also known that gold atoms share the $6s^1$ atomic orbital. The single valence electron can combine with the open-shell orbital to form a closed-shell orbital when a gold atom is added to the open-shell cluster, affording $Au_nP_2^-$ (n = 1, 3, 5, 7). This removes one occupied molecular orbital.

3.2.3. Natural bond orbital (NBO) analysis

We have summarized Natural population analysis (NPA) and natural electron configuration (NEC) from NBO [80,81] analysis of the global minima within the low-lying isomers of the $Au_nP_2^-$ (n = 1–8) clusters in Fig. 6. The atomic charge is labeled in square brackets above the atom, and the electron configuration of each atom is provided below the atom. Atoms are also labeled in proper sequence.

Structures with high symmetry have some of the same types of gold or phosphorus atoms. The classification is shown in the figure. The species have 1, 2, 2, 4, 3, 4, 4, 3, and 4 types of Au atoms from n = 2 to 8, respectively (two isomers for n = 6). When n is less than or equal to 5, the two bonded phosphorus atoms share no more than 0.5 units of charge, except for AuP_2^-. When n is greater than 5, the two phosphorus atoms separated from each other share more charge than all of the other gold

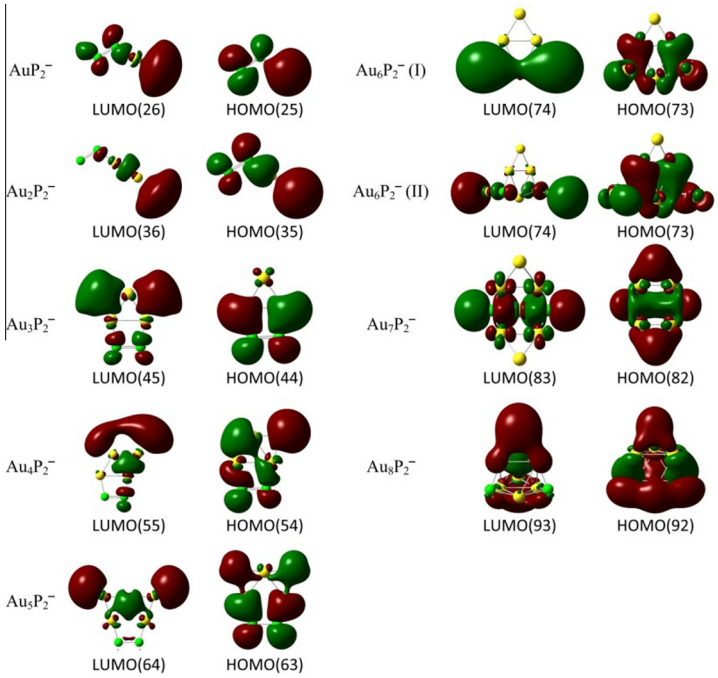

Fig. 5. Frontier molecular orbitals of $Au_nP_2^-$ (n = 1–8).

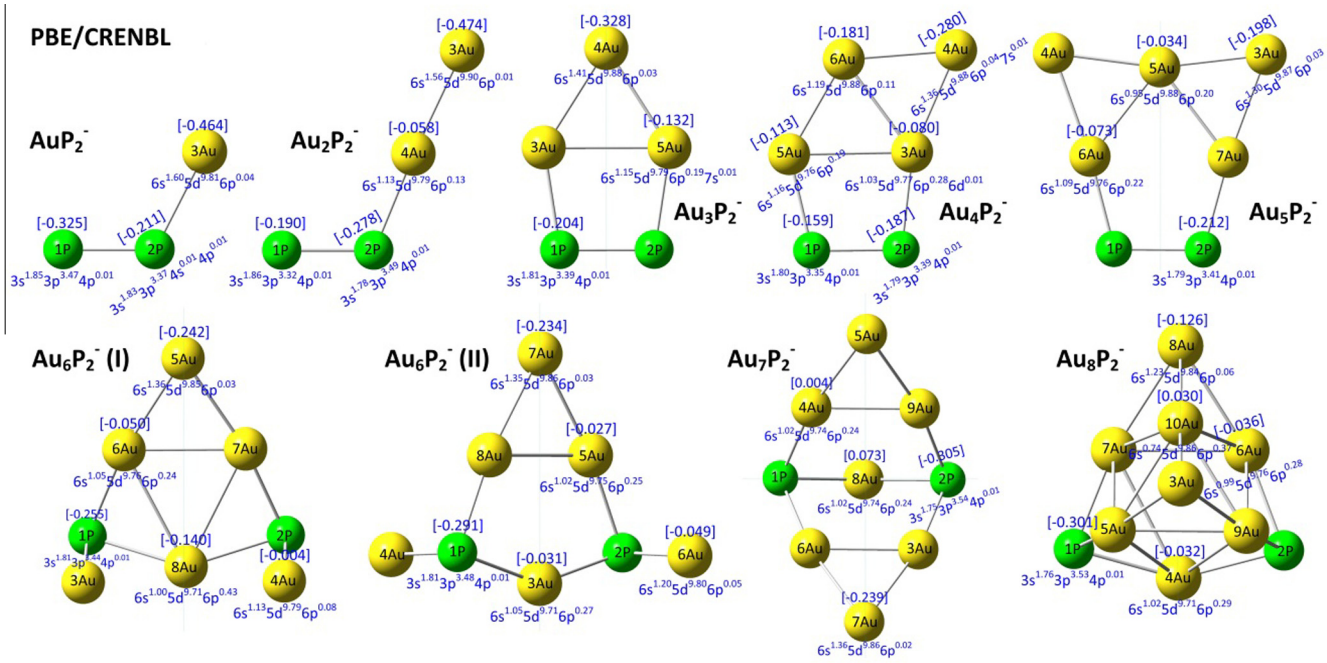

Fig. 6. Natural population analysis (NPA) (a.u.) and natural electron configuration (NEC) of $Au_nP_2^-$ at the PBE/CRENBL level.

atoms. In addition, the overall negative charge distribution of clusters prefers to localize on the apex atoms rather than the edge atoms. One possible explanation is that the repulsive interaction of the outside valence electrons stabilizes the structures with the weakest repulsive interaction. $Au_6P_2^-$ is unique because it possesses two global minima that are mutual cis–trans isomers. We searched for insights to better understand the difference between these isomers. The steric hindrance effect of $Au_6P_2^-$ (II) is smaller than that of $Au_6P_2^-$ (I), and the phosphorus atoms share more natural charge. In $Au_7P_2^-$, 5 of the 7 gold atoms are adjacent to phosphorus and have a positive natural charge. This result means that the gold atoms act as an electron donor, losing an electron to their surrounding environment. Additionally, the other four electron acceptors are in apex positions. $Au_8P_2^-$, a 3D pyramidal configuration with C_{2v} symmetry, as mentioned above, has 4 types of Au atoms, 5–6–7–9, 3–8, 4 and 10. As shown, the four apex atoms of the pyramidal structure possess a higher charge than the edge atoms. Au10 possesses a positive charge of 0.030, indicating that it is an electron donor.

To better understand the above phenomenon, the NEC is also considered. As shown in Fig. 6, the electrons on the phosphorus atom are mainly in the 3s and 3p orbitals; the 4p orbital also

accepts small amount of charge. The electrons on the gold atoms are mainly concentrated in the 5d and 6s orbitals. Due to the strong relativistic effects of the heavy gold atoms contracting the 6s orbital, the energies of the 5d and 6s orbitals reverse as the valence electron configurations of gold atom is $5d^{10}6s^1$, and these orbitals hybridize with each other on gold atoms. Au5 of $Au_3P_2^-$ and Au4 of $Au_4P_2^-$ also have electrons that localize due to the explicit interaction of the repulsive interactions of electrons and the attractive interactions of nuclei.

4. Conclusions

In conclusion, we have presented a theoretical study on the structural and electronic properties of $Au_nP_2^-$ clusters in the size range of 1–8 atoms. The results indicate that the structures of $Au_nP_2^-$ clusters have one clear global minimum structure, with the exception of $Au_6P_2^-$ due to its two cis–trans isomers of similar energies. In particular, the global minimum of $Au_8P_2^-$ is a pyramid-shaped structure that is similar to that of Au_{20}^- and with potential novel optical and catalytic properties, providing a possible new direction for materials synthesis and catalysis. Relativistic stability analysis testifies that the P atom impurity can in fact enhance the stabilities of pure gold clusters. The dual-phosphorus dopants, which are quite different from the pure clusters, exhibit preference in the evolutionary path for small to medium-sized clusters. The mechanism for the evolution of the $Au_nP_2^-$ clusters shows different growth paths than pure gold clusters or single-phosphorus-doped gold clusters. The 2D–3D structural transition of $Au_nP_2^-$ is much clearer and faster than that of the pure gold clusters. The transition of the structure of the species ($Au_nP_2^-$) from 2D to 3D occurs at $n = 6$, while the corresponding value is 12 for pure anionic gold clusters (Au_n^-). Meanwhile, single-phosphorus-doped gold clusters (Au_nP^-) exhibit an even–odd oscillation in their 2D/3D transition. Molecular orbital analysis was used to identify open- and closed-shell rules for studying the evolution of $Au_nP_2^-$. NPA suggests that the atoms at the apex have more anionic electrons than the atoms at the edges for stabilizing the structures with the weakest repulsive interactions. Separated phosphorus atoms possess more electrons than connected phosphorus atoms and higher charge than the corresponding gold atoms. All electrons localize in the 3s and 3p orbitals of phosphorus and the 6s and 5d orbitals of gold atoms. The level inversion and orbital hybridization of the 5d and 6s orbitals shown in NEC evidence the relativistic effects of the gold atoms.

Experimental studies of phosphorus-doped clusters remain necessary to determine their sizes and shapes, as our study provides only theoretically simulated photoelectron spectra. In our future work, we will investigate medium- to large-sized phosphorus-doped clusters and pay more attention to possible notable characteristics of the phosphorus dopants.

Conflict of interest

The authors declared no conflict of interest in this paper.

Acknowledgments

The study was supported by grants from the National Natural Science Foundation of China (Grant no. 21403244 and 21133008), and the National High Technology Research and Development Program of China (863 Program) (Grant no. 2014AA06A501). Acknowledgement is also made to the "Thousand Youth Talents Plan" and "Interdisciplinary and Cooperative Team" of CAS. The computation was performed in EMSL, a national scientific user facility sponsored by the department of Energy's Office of Biological and Environmental Research and located at Pacific Northwest National Laboratory (PNNL). PNNL is a multi-program national laboratory operated for the DOE by Battelle. Part of the computation was performed at the Supercomputing Center of the Chinese Academy of Sciences and Supercomputing Center of USTC.

Appendix A. Supplementary data

Supplementary data associated with this article can be found, in the online version, at http://dx.doi.org/10.1016/j.chemphys.2015.04.019.

References

[1] P. Pyykkö, Angew. Chem. Int. Ed. 43 (2004) 4412.
[2] P. Pyykkö, Inorg. Chim. Acta 358 (2005) 4113.
[3] P. Pyykkö, Chem. Soc. Rev. 37 (2008) 1967.
[4] M. Haruta, Catal. Today 36 (1997) 153.
[5] A.A. Herzing, C.J. Kiely, A.F. Carley, P. Landon, G.J. Hutchings, Science 321 (2008) 1331.
[6] H. Häkkinen, M. Moseler, U. Landman, Phys. Rev. Lett. 89 (2002) 033401.
[7] F. Furche, R. Ahlrichs, P. Weis, C. Jacob, S. Gilb, T. Bierweiler, M.M. Kappes, J. Chem. Phys. 117 (2002) 6982.
[8] H. Häkkinen, B. Yoon, U. Landman, X. Li, H.J. Zhai, L.S. Wang, J. Phys. Chem. A 107 (2003) 6168.
[9] S. Bulusu, X. Li, L.S. Wang, X.C. Zeng, Proc. Natl. Acad. Sci. U.S.A. 103 (2006) 8326.
[10] X. Xing, B. Yoon, U. Landman, J.H. Parks, Phys. Rev. B 74 (2006) 165423.
[11] J. Li, X. Li, H.J. Zhai, L.S. Wang, Science 299 (2003) 864.
[12] P. Gruene, D.M. Rayner, B. Redlich, A.F.G. van der Meer, J.T. Lyon, G. Meijer, A. Fielicke, Science 321 (2008) 674.
[13] B. Yoon, P. Koskinen, B. Huber, O. Kostko, B. von Issendorff, H. Hakkinen, M. Moseler, U. Landman, ChemPhysChem 8 (2007) 157.
[14] S. Bulusu, X. Li, L.S. Wang, X.C. Zeng, J. Phys. Chem. C 111 (2007) 4190.
[15] M. Ji, X. Gu, X. Li, X.G. Gong, J. Li, L.S. Wang, Angew. Chem. Int. Ed. 44 (2005) 7119.
[16] A.F. Jalbout, F.F. Contreras-Torres, L.A. Perez, I.L. Garzón, J. Phys. Chem. A 112 (2008) 353.
[17] A. Lechtken, D. Schooss, J.R. Stairs, M.N. Blom, F. Furche, N. Morgner, O. Kostko, B. von Issendorff, M.M. Kappes, Angew. Chem. Int. Ed. 46 (2007) 2944.
[18] X. Gu, S. Bulusu, X. Li, X.C. Zeng, J. Li, X.G. Gong, L.S. Wang, J. Phys. Chem. C 111 (2007) 8228.
[19] I.E. Santizo, F. Hidalgo, L.A. Perez, C. Noguez, I.L. Garzón, J. Phys. Chem. C 112 (2008) 17533.
[20] I.L. Garzón, K. Michaelian, M.R. Beltrán, A. Posada-Amarillas, P. Ordejón, E. Artacho, D. Sánchez-Portal, J.M. Soler, Phys. Rev. Lett. 81 (1998) 1600.
[21] H. Häkkinen, M. Moseler, O. Kostko, N. Morgner, M.A. Hoffmann, B. von Issendorff, Phys. Rev. Lett. 93 (2004) 093401.
[22] W. Huang, M. Ji, C.D. Dong, X. Gu, L.M. Wang, X.G. Gong, L.S. Wang, ACS Nano 2 (2008) 897.
[23] N. Shao, W. Huang, Y. Gao, L.M. Wang, X. Li, L.S. Wang, X.C. Zeng, J. Am. Chem. Soc. 132 (2010) 6596.
[24] W. Huang, L.S. Wang, Phys. Rev. Lett. 102 (2009) 153401.
[25] W. Huang, H.J. Zhai, L.S. Wang, J. Am. Chem. Soc. 132 (2010) 4344.
[26] W. Bouwen, F. Vanhoutte, F. Despa, S. Bouckaert, S. Neukermans, L.T. Kuhn, H. Weidele, P. Lievens, R.E. Silverans, Chem. Phys. Lett. 314 (1999) 227.
[27] M. Heinebrodt, N. Malinowski, F. Tast, W. Branz, I.M.L. Billas, T.P. Martin, J. Chem. Phys. 110 (1999) 9915.
[28] K. Koyasu, M. Mitsui, A. Nakajima, K. Kaya, Chem. Phys. Lett. 358 (2002) 224.
[29] B.R. Sahu, G. Maofa, L. Kleinman, Phys. Rev. B 67 (2003) 115420.
[30] K. Koszinowski, D. Schroder, H. Schwarz, ChemPhysChem 4 (2003) 1233.
[31] H. Häkkinen, W. Abbet, A. Sanchez, U. Heiz, U. Landman, Angew. Chem. Int. Ed. 42 (2003) 1297.
[32] E. Janssens, H. Tanaka, S. Neukermans, R.E. Silverans, P. Lievens, New J. Phys. 5 (2003) 46.1.
[33] H. Tanaka, S. Neukermans, E. Janssens, R.E. Silverans, P. Lievens, J. Am. Chem. Soc. 125 (2003) 2862.
[34] L. Gagliardi, J. Am. Chem. Soc. 125 (2003) 7504.
[35] H. Tanaka, S. Neukermans, E. Janssens, R.E. Silverans, P. Lievens, J. Chem. Phys. 119 (2003) 7115.
[36] H.J. Zhai, J. Li, L.S. Wang, J. Chem. Phys. 121 (2004) 8369.
[37] E. Janssens, H. Tanaka, S. Neukermans, R.E. Silverans, P. Lievens, Phys. Rev. B 69 (2004) 085402.
[38] D.W. Yuan, Y. Wang, Z. Zeng, J. Chem. Phys. 122 (2005) 114310.
[39] M.B. Torres, E.M. Fernandez, L.C. Balbas, Phys. Rev. B 71 (2005) 115412.
[40] H. Wen, Y.R. Liu, T. Huang, K.M. Xu, W.J. Zhang, W. Huang, L.S. Wang, J. Chem. Phys. 138 (2013) 174303.
[41] L.M. Wang, L.S. Wang, Nanoscale 4 (2012) 4038.
[42] L.L. Yan, Y.R. Liu, T. Huang, S. Jiang, H. Wen, Y.B. Gai, W.J. Zhang, W. Huang, J. Chem. Phys. 139 (2013) 244312.

[43] W. Huang, L.S. Wang, Phys. Chem. Chem. Phys. 11 (2009) 2663.
[44] H. Wen, Y.R. Liu, K.M. Xu, T. Huang, C.J. Hu, W.J. Zhang, W. Huang, RSC Adv. 4 (2014) 15066.
[45] M. Götz, M. Willis, A.K. Kandalam, G.F. Ganteför, P. Jena, ChemPhysChem 11 (2010) 853.
[46] F. Buendia, M.R. Beltrán, X. Zhang, G. Liu, A. Buytendyk, K. Bowen, Phys. Chem. Chem. Phys. (2015), http://dx.doi.org/10.1039/C5CP00115C.
[47] E.J. Fernandez, A. Laguna, M.E. Olmos, J. Chil. Chem. Soc. 52 (2007) 1200.
[48] A.I. Kozlov, A.P. Kozlova, H.C. Liu, Y. Iwasawa, Appl. Catal. A: Gen. 182 (1999) 9.
[49] W. Jeitschko, M.H. Moller, Acta Crystallog. Sect. B: Struct. Sci. 35 (1979) 573.
[50] M. Eschen, W. Jeitschko, J. Solid State Chem. 165 (2002) 238.
[51] V.G. Weizer, N.S. Fatemi, J. Appl. Phys. 69 (1991) 8253.
[52] A.E. Henkes, Y. Vasquez, R.E. Schaak, J. Am. Chem. Soc. 129 (2007) 1896.
[53] Z.Y. Liu, R.B. Huang, L.S. Zheng, Chem. J. Chin. Univ. 18 (1997) 293.
[54] N.R. Panyala, E.M. Peña-Méndez, J. Havel, Rapid Commun. Mass Spectrom. 26 (2012) 1100.
[55] S. Carenco, I. Florea, O. Ersen, C. Boissiere, N. Mezailles, C. Sanchez, New J. Chem. 37 (2013) 1231.
[56] X.D. Wen, T.J. Cahill, R. Hoffmann, J. Am. Chem. Soc. 131 (2009) 2199.
[57] Y. Li, Y.P. Cao, Y.F. Li, S.P. Shi, X.Y. Kuang, Eur. Phys. J. D 66 (2012) 10.
[58] G.F. Zhao, Y.L. Wang, J.M. Sun, Y.X. Wang, Acta Phys.-Chim. Sin. 28 (2012) 1355.
[59] M. Zhang, S. Chen, Q.M. Deng, L.M. He, L.N. Zhao, Y.H. Luo, Eur. Phys. J. D 58 (2010) 117.
[60] C. Majumder, A. Kandalam, P. Jena, Phys. Rev. B 74 (2006) 205437.
[61] K.M. Xu, T. Huang, H. Wen, Y.R. Liu, Y.B. Gai, W.J. Zhang, W. Huang, RSC Adv. 3 (2013) 24492.
[62] S.H. Yoo, X.C. Zeng, Angew. Chem. Int. Ed. 44 (2005) 1491.
[63] D.J. Wales, J.P.K. Doye, J. Phys. Chem. A 101 (1997) 5111.
[64] W. Huang, R. Pal, L.M. Wang, X.C. Zeng, L.S. Wang, J. Chem. Phys. 132 (2010) 054305.
[65] S. Yoo, X.C. Zeng, J. Chem. Phys. 119 (2003) 1442.
[66] Y.R. Liu, H. Wen, T. Huang, X.X. Lin, Y.B. Gai, C.J. Hu, W.J. Zhang, W. Huang, J. Phys. Chem. A 118 (2014) 508.
[67] J.P. Perdew, K. Bruke, M. Ernzerhof, Phys. Rev. Lett. 77 (1996) 3865.
[68] A.D. Becke, J. Chem. Phys. 98 (1993) 5648.
[69] C.T. Lee, W.T. Yang, R.G. Parr, Phys. Rev. B 37 (1988) 785.
[70] A.D. Becke, Phys. Rev. A 38 (1988) 3098.
[71] R.A. Kendall, E. Apra, D.E. Bernholdt, E.J. Bylaska, M. Dupuis, G.I. Fann, R.J. Harrison, J.L. Ju, J.A. Nichols, J. Nieplocha, T.P. Straatsma, T.L. Windus, A.T. Wong, Comput. Phys. Commun. 128 (2000) 260.
[72] E.J. Bylaska, W.A. de Jong, N. Govind, K. Kowalski, T.P. Straatsma, M. Valiev, D. Wang, E. Apra, T.L. Windus, J. Hammond, P. Nichols, S. Hirata, M.T. Hackler, Y. Zhao, P.D. Fan, R.J. Harrison, M. Dupuis, D.M.A. Smith, J. Nieplocha, V. Tipparaju, M. Krishnan, Q. Wu, T. Van Voorhis, A. A. Auer, M. Nooijen, E. Brown, G. Cisneros, G.I. Fann, H. Fruchtl, J. Garza, K. Hirao, R. Kendall, J.A. Nichols, K. Tsemekhman, K. Wolinski, J. Anchell, D. Bernholdt, P. Borowski, T. Clark, D. Clerc, H. Dachsel, M. Deegan, K. Dyall, D. Elwood, E. Glendening, M. Gutowski, A. Hess, J. Jaffe, B. Johnson, J. Ju, R. Kobayashi, R. Kutteh, Z. Lin, R. Littlefield, X. Long, B. Meng, T. Nakajima, S. Niu, L. Pollack, M. Rosing, G. Sandrone, M. Stave, H. Taylor, G. Thomas, J. van Lenthe, A. Wong, Z. Zhang, NWChem, A Computational Chemistry Package for Parallel Computers, Version 5.1, Pacific Northwest National Laboratory, Richland, 2009.
[73] C. Adamo, V. Barone, J. Chem. Phys. 110 (1999) 6158.
[74] R.B. Ross, J.M. Powers, T. Atashroo, W.C. Ermler, L.A. Lajohn, P.A. Christiansen, J. Chem. Phys. 93 (1990) 6654.
[75] W. Huang, S. Bulusu, R. Pal, X.C. Zeng, L.S. Wang, ACS Nano 3 (2009) 1225.
[76] W. Huang, S. Bulusu, R. Pal, X.C. Zeng, L.S. Wang, J. Chem. Phys. 131 (2009) 234305.
[77] L.M. Wang, R. Pal, W. Huang, X.C. Zeng, L.S. Wang, J. Chem. Phys. 132 (2010) 114306.
[78] R. Pal, L.M. Wang, W. Huang, L.S. Wang, X.C. Zeng, J. Chem. Phys. 134 (2011) 054306.
[79] R. Pal, W. Huang, Y.L. Wang, H.S. Hu, S. Bulusu, X.G. Xiong, J. Li, L.S. Wang, X.C. Zeng, J. Phys. Chem. Lett. 2 (2011) 2288.
[80] A.E. Reed, F. Weinhold, J. Chem. Phys. 78 (1983) 4066.
[81] A.E. Reed, L.A. Curtiss, F. Weinhold, Chem. Rev. 88 (1988) 899.
[82] A.E. Reed, R.B. Weinstock, F. Weinhold, J. Chem. Phys. 83 (1985) 735.
[83] H. Häkkinen, U. Landman, Phys. Rev. B 62 (2000) R2287.
[84] K.M. Xu, S. Jiang, Y.P. Zhu, T. Huang, Y.R. Liu, Y. Zhang, Y.Z. Lv, W. Huang, RSC Adv. 5 (2015) 26071.
[85] B. Assadollahzadeh, P. Schwerdtfeger, J. Chem. Phys. 131 (2009) 064306.